

Dynamic Mechanical Behavior of High-Density Polyethylene/Ethylene Vinyl Acetate Copolymer Blends: The Effects of the Blend Ratio, Reactive Compatibilization, and Dynamic Vulcanization

Biju John,¹ K. T. Varughese,² Zachariah Oommen,³ Petra Pötschke,⁴ Sabu Thomas¹

¹ School of Chemical Sciences, Mahatma Gandhi University, Priyadarshini Hills P.O., Kottayam, Kerala, India, 686560

² Polymer Laboratory, Central Power Research Institute, Bangalore, India, 560080

³ Department of Chemistry, CMS College, Kottayam, Kerala, India, 686001

⁴ Department of Polymer Reactions and Blends, Institute of Polymer Research Dresden, Dresden, Germany

Received 27 June 2001; accepted 17 April 2002

ABSTRACT: The effects of the blend ratio, reactive compatibilization, and dynamic vulcanization on the dynamic mechanical properties of high-density polyethylene (HDPE)/ethylene vinyl acetate (EVA) blends have been analyzed at different temperatures. The storage modulus of the blend decreases with an increase in the EVA content. The loss factor curve shows two peaks, corresponding to the transitions of HDPE and EVA, indicating the incompatibility of the blend system. Attempts have been made to correlate the observed viscoelastic properties of the blends with the blend morphology. Various composite models have been used to predict the dynamic mechanical data. The experimental values are close to those of the Halpin–Tsai model above 50 wt % EVA and close to those of the Coran model up to 50 wt % EVA in the blend. For the Takayanagi model, the theoretical value is in good agreement with the experimental value for a 70/30 HDPE/EVA blend. The area under the loss modulus/temperature curve (LA) has been analyzed with the integration method from the experimental curve and has been compared with that obtained from group contribution analysis. The LA values calculated with group contribution analysis are lower than those calculated with the integration method. The addition of a maleic-modified polyethylene

compatibilizer increases the storage modulus, loss modulus, and loss factor values of the system, and this is due to the finer dispersion of the EVA domains in the HDPE matrix upon compatibilization. For 70/30 and 50/50 blends, the addition of a maleic-modified polyethylene compatibilizer shifts the relaxation temperature of both HDPE and EVA to a lower temperature, and this indicates increased interdiffusion of the two phases at the interface upon compatibilization. However, for a 30/70 HDPE/EVA blend, the addition of a compatibilizer does not change the relaxation temperature, and this may be due to the cocontinuous morphology of the blends. The dynamic vulcanization of the EVA phase with dicumyl peroxide results in an increase in both the storage and loss moduli of the blends. A significant increase in the relaxation temperature of EVA and a broadening of the relaxation peaks occur during dynamic vulcanization, and this indicates the increased interaction between the two phases. © 2003 Wiley Periodicals, Inc. *J Appl Polym Sci* 87: 2083–2099, 2003

Key words: polyethylene (PE); blends; mechanical properties

INTRODUCTION

During the last few decades, the commercial importance of polymer blends has increased because of the possibility of attaining a wide range of properties through blending. Although it is possible to combine the properties of two or more polymers through blending, many of these blends are immiscible and incompatible. These immiscible blends exhibit poor mechanical properties because of the lack of physical and chemical interaction across the phase boundaries and poor interfacial adhesion.

Dynamic mechanical analysis can often be used to characterize the miscibility between two polymers. The dynamic mechanical properties, such as the storage modulus (G'), loss modulus (G''), and loss factor ($\tan \delta$), of polymer blends depend on the structure, crystallinity, extent of crosslinking,¹ and so forth. Cho et al.² studied the dynamic mechanical properties of blends of linear low-density polyethylene (PE) and ethylene-propylene-butene-1 terpolymer. The α , β , and γ dynamic mechanical relaxations, which may arise because of the constituents, give valuable information on the state of miscibility in the amorphous and crystalline phases. Karger-Kocsis and Kiss³ investigated the effect of morphology on the dynamic mechanical properties of PP/EPDM blends. They found that G' of blends decreases with an increase in the concentration of EPDM. The presence of two separate

Correspondence to: S. Thomas (sabut@vsnl.com).

damping peaks of blend components at their original positions in the dynamic mechanical spectrum suggests that the blend is incompatible and has a two-phase morphology. Thomas et al.⁴ studied the dynamic mechanical behavior of NBR/ethylene vinyl acetate (EVA) blends with special reference to the effect of the blend ratio, dynamic crosslinking, and temperature. The damping properties of the blends decrease with an increase in the EVA concentration. The change in the dynamic properties was correlated with the morphology of the system, and various theoretical models were used to predict the dynamic mechanical behavior of the blends.

The properties of immiscible polymer blends can be improved by the addition of compatibilizers or interfacial agents.⁵ A suitably selected compatibilizer will be located at the interface between the two components and consequently reduce the interfacial tension and improve the interfacial adhesion and, therefore, the mechanical properties. The effects of compatibilization on the dynamic mechanical properties of various polymer blends have been reported. The compatibilization of high-density polyethylene (HDPE)/polyisoprene (PI) blends with PE/PI copolymers was investigated by Zhang et al.⁶ The dynamic mechanical studies showed that with the addition of the copolymer, both the glass-transition temperature (T_g) of the PI component and the relaxation of HDPE shifted to lower temperatures, demonstrating the enhanced penetration of the two components.

The effects of dynamic vulcanization on the dynamic mechanical properties of polymer blends have been reported. The effects of the blend ratio and dynamic crosslinking of the elastomer phase on the dynamic mechanical properties of PP/EVA blends were studied by Thomas and George.⁷ The dynamic mechanical properties of both uncrosslinked and dynamically crosslinked blends indicate two separate transitions corresponding to EVA and PP phases, indicating the immiscibility of the system. Dynamic crosslinking results in the broadening of peaks, which indicates some degree of compatibility attained during crosslinking. Koshy et al.⁸ reported on the thermal, crystallization, and dynamic mechanical properties of natural rubber/EVA blends. The differential scanning calorimetry and dynamic mechanical thermal analysis results show that the blend components are incompatible in the crosslinked and uncrosslinked states. The predominant crosslinking of the natural rubber phase as a result of the addition of sulfur or mixed crosslinking agents can be analyzed by the shift in T_g of the natural rubber phase toward higher temperatures.

The dynamic mechanical behavior of thermoplastic elastomer blends was recently reported by this laboratory.⁹ The dynamic mechanical properties of isotactic polypropylene/nitrile rubber blends were investigated by George et al.⁹ The effects of the blend ratio,

reactive compatibilization, and dynamic crosslinking on the dynamic mechanical properties were analyzed. The addition of maleic- and phenolic-modified polypropylene improved G' of the blends. The enhancement in G' and the change in the domain size of the dispersed NBR particles upon compatibilization were explained.

Blends of HDPE with EVA possess excellent processing characteristics, the mechanical properties of HDPE, and the flexibility and environmental stress-crack resistance of EVA. Recently, the morphology and mechanical properties of these blends were reported by this laboratory.¹⁰ In this article, we report on the dynamic mechanical properties of HDPE/EVA blends. The effects of the blend ratio, dynamic crosslinking, and reactive compatibilization on the dynamic mechanical properties have been studied. Attempts have been made to correlate the dynamic mechanical properties with the morphology of the blend. Finally, the experimental dynamic mechanical properties are compared with theoretical models.

EXPERIMENTAL

Materials

HDPE (Relene, M60 200) with a density of 0.96 g/cc and a melt flow index of 20 g/10 min was obtained from Reliance Industries, Ltd. (Gujarat, India). EVA (Pilene 1802) with a vinyl acetate content of 18%, a density of 0.93 g/cc, and a melt flow index of 2 g/10 min was obtained from NOCIL (Mumbai, India).

Maleic-modified polyethylene (MA-PE) was prepared by the melt blending of HDPE (100 g) with maleic anhydride (MA; 5 g) and dicumyl peroxide (DCP; 0.5 g).¹¹ The melt mixing was carried out in a Brabender plasticorder at 180°C and 60 rpm. The modified materials were removed from the mixer and cut into small pieces for use as compatibilizers.

Preparation of the blends

Blends were prepared in a laboratory-type Brabender plasticorder (45-cc capacity) by the melt mixing of the components at a temperature of 160°C and at a rotor speed of 60 rpm. HDPE was melted for 2 min, and then EVA was added. The mixing was continued for 5 min. Sheets 2 mm thick were prepared via compression molding.

Blend morphology

The morphology studies of the blends were carried out with a scanning electron microscope (JSM 5600) after the sputter coating of the samples with gold. The compression-molded samples were fractured under liquid nitrogen, and the EVA phase was preferentially extracted from the samples with carbon tetrachloride at room temperature for 5 days.

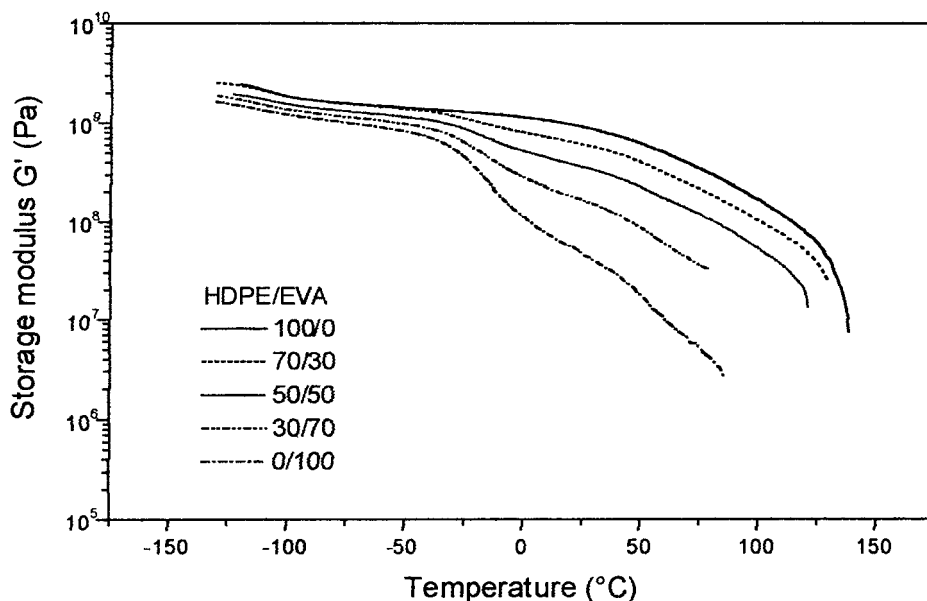


Figure 1 Dependence of G' on the temperature of HDPE/EVA blends.

From the scanning electron microscopy results, the particle size determination was carried out by the measurement of the domain diameter. From this, the number-average (D_n), weight-average (D_w), and volume-average (D_v) domain diameters were calculated:

$$D_n = \frac{\sum N_i D_i}{\sum N_i} \quad (1)$$

$$D_w = \frac{\sum N_i D_i^2}{\sum N_i D_i} \quad (2)$$

$$D_v = \frac{\sum N_i D_i^4}{\sum N_i D_i^3} \quad (3)$$

Dynamic mechanical testing

The dynamic mechanical behavior of the blends was studied by means of an advanced rheometric expansion system in the oscillation mode at a frequency of 10 Hz and at a strain rate of 0.5–0.7%. The temperature range used was -130 to 150°C in an atmosphere of N_2 . The samples were cut from compression-molded specimens about 2 mm thick and 12 mm wide. Before the measurements were begun, the samples were pre-cooled at -130°C for 5 min. The heating rate was 5 K/min, and the measurement interval was 15 s.

RESULTS AND DISCUSSION

Effect of the blend ratio

The dynamic mechanical properties, including G' , G'' , and $\tan \delta$ or damping of the pure components and

blends, were evaluated from -130 to $+150^\circ\text{C}$. Figures 1–3 represent the variations of $\tan \delta$, G'' , and G' with temperature. HDPE shows two relaxations, an α relaxation at $+80^\circ\text{C}$ and a γ relaxation at -110°C . The α relaxation is associated with the chain segment mobility in the crystalline phases—probably the reorientation of defect areas in crystals. The α relaxation appears to be a composite process¹² of two transitions labeled α and α' (ca. 120°C). The γ relaxation is associated with the amorphous phase. Therefore, as the crystallinity of the substance decreases, the γ relaxation increases, and it corresponds to T_g of HDPE.

Because EVA is a copolymer of ethylene and vinyl acetate, it exhibits typical transitions of PE as well: a low-temperature transition at a temperature lower than the starting measurement temperature of -130°C and a relaxation at -15°C (the α relaxation is overlapped by the melting of EVA at about 90°C). The peak at about -15°C is described in the literature¹³ as a β transition of branched PE (the relaxation temperature of EVA obtained from the G'' -temperature curve is lower than that obtained from the $\tan \delta$ curve; the relaxation temperature from the G'' -temperature curve is -24°C , and that from the $\tan \delta$ curve is -15°C). It corresponds to T_g of EVA, and in the figures it is marked as a relaxation of EVA. This β relaxation is caused by the movement of alkyl side chains of the PE part of the copolymer, and the temperature of the relaxation is independent of the vinyl acetate content as long as the copolymer is crystalline. In HDPE, this β transition is not visible because of the absence of branches.

G' of EVA is lower than that of HDPE over the entire temperature range (Fig. 1). G' of EVA shows a

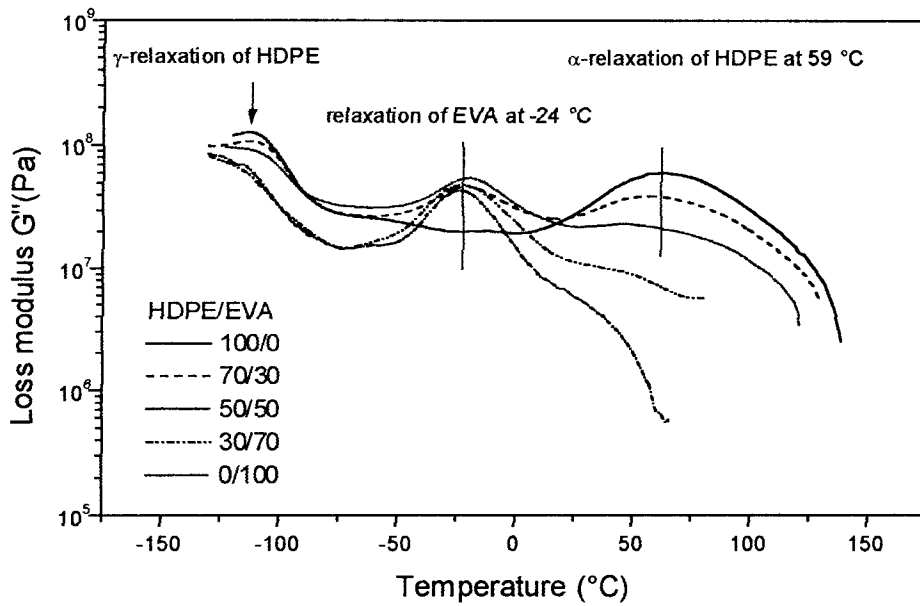


Figure 2 Dependence of G'' on the temperature of HDPE/EVA blends.

drastic fall around the T_g region, but for HDPE, because of its crystalline nature, the drop is at a lower rate. This is because in crystalline materials, during the transition, only the amorphous part undergoes segmental motion, whereas the crystalline region remains a crystalline solid until its temperature of melting. As the amount of EVA in the blend increases, the G' values decrease over the whole temperature range.

For HDPE, 70/30 HDPE/EVA, and 50/50 HDPE/EVA, the α relaxation of HDPE (G'' maximum) occurs at 59, 56, and 50°C, respectively (Fig. 2). The G'' -temperature curves show two relaxation peaks corre-

sponding to HDPE and EVA components in the blend. As the EVA content in the blend increases, the relaxation temperature decreases only slightly. For EVA, the relaxation (G'' maximum) occurs at -24°C, and with an increase in the amount of HDPE in the blend, there is only a marginal increase in the relaxation temperature.

The miscibility of the blend components can be predicted with dynamic mechanical data.^{5,7} Generally, for an immiscible blend, the $\tan \delta$ -temperature curve shows the presence of two $\tan \delta$ damping peaks corresponding to T_g 's of individual polymers.⁵ For mis-

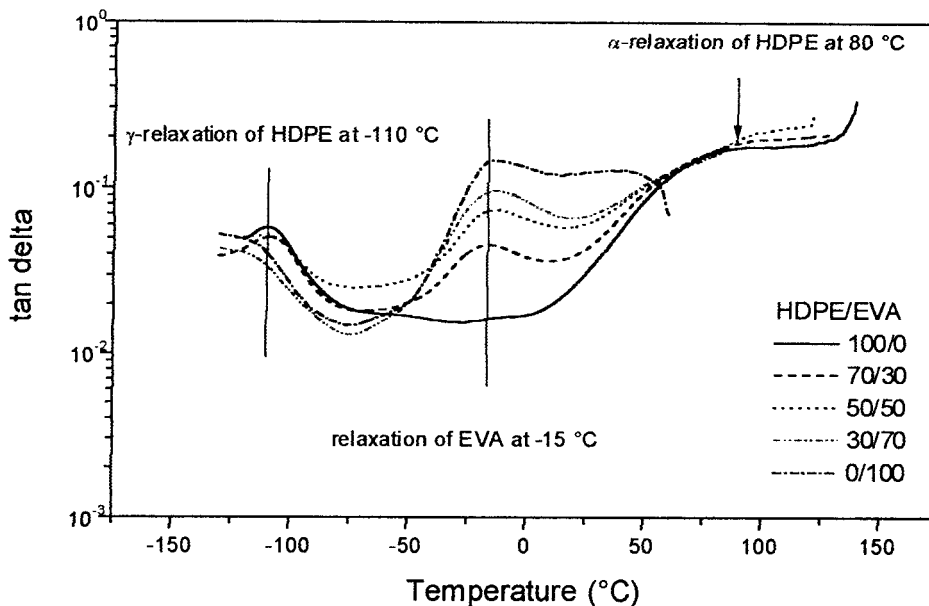


Figure 3 Dependence of $\tan \delta$ on the temperature of HDPE/EVA blends.

TABLE I
 T_g 's of HDPE and EVA

| Sample | $\tan \delta_{\max}$ ($^{\circ}\text{C}$; T_g HDPE) | $\tan \delta_{\max}$ ($^{\circ}\text{C}$; T_g EVA) |
|----------------------|--|---|
| HDPE | -110.2 | — |
| 70/30 HDPE/EVA blend | -108.9 | -16.4 |
| 50/50 HDPE/EVA blend | -116.4 | -15.3 |
| 30/70 HDPE/EVA blend | — | -14.3 |
| EVA | — | -14.8 |

cible blends, the curve shows only a single peak¹⁴ between the transition temperatures of the component polymers. However, for a partially miscible system,¹⁵ a broadening of the transition occurs, and the T_g values are shifted to higher or lower temperatures as a function of composition. The HDPE/EVA blends exhibit two distinct peaks corresponding to the individual polymers, as can be seen in a plot of the $\tan \delta$ -temperature curve (Fig. 3). Two separate peaks corresponding to the T_g 's of HDPE (-110°C) and EVA (-15°C) indicate the immiscibility and incompatibility of the system.

EVA has a higher damping intensity than HDPE because of its rubbery nature. During blending, the T_g values corresponding to HDPE and EVA components were shifted to lower temperatures. The shift in the T_g values of HDPE and EVA is given in Table I. The damping of the blends at -15°C increases with an increase in the concentration of EVA, and it is evident in Figure 3. The increase in the damping behavior with an increase in the EVA content is due to the reduction in the crystalline volume of the system with an in-

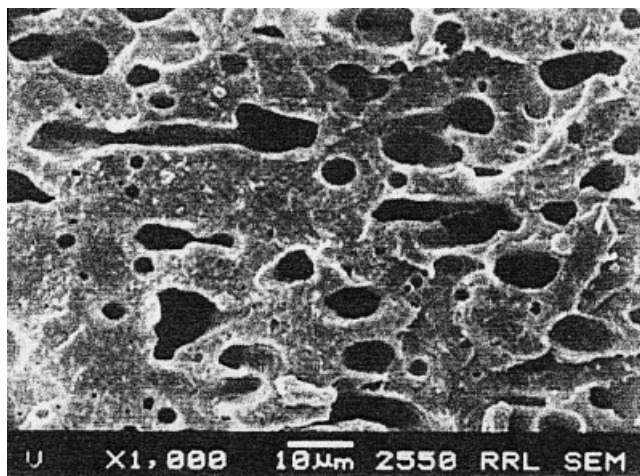


Figure 5 Scanning electron micrograph of 70/30 HDPE/EVA blends.

crease in the concentration of EVA, the damping of which is higher than that of HDPE.

The variation of $\tan \delta$ and G' of the blends with the EVA content in the blend at $-25 \pm 1^{\circ}\text{C}$ is given in Figure 4 (the relaxation of EVA occurs at -24°C , and there is a rapid fall in the G' values around this temperature). From the figure, it is obvious that the variation of $\tan \delta$ is more pronounced at higher concentrations of EVA in comparison with that at lower concentrations in the blend. The variation of $\tan \delta$ with the concentration of EVA can be explained in terms of the morphology of the blend. Figures 5-7 provide the scanning electron micrographs of 70/30, 50/50, and 30/70 HDPE/EVA blends. In the 70/30 blend, the

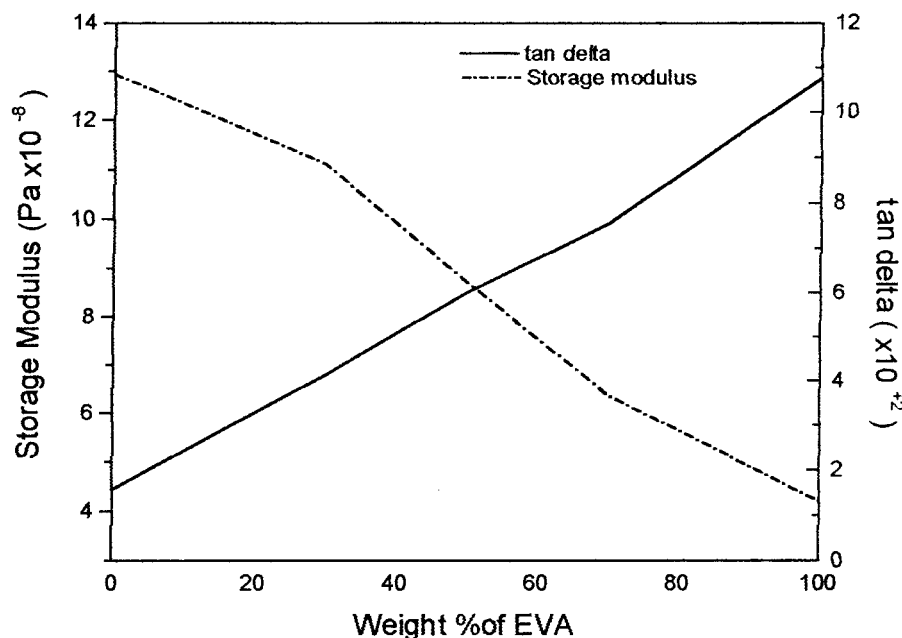


Figure 4 Dependence of G' and $\tan \delta$ on the weight percentage of EVA in the blend at -25°C .

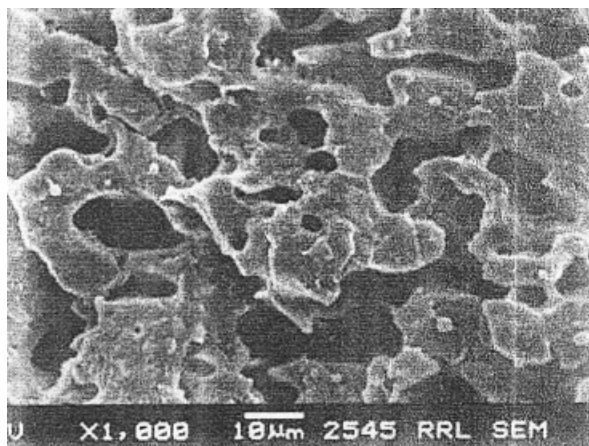


Figure 6 Scanning electron micrograph of 50/50 HDPE/EVA blends.

EVA phase is dispersed as spherical domains in the continuous HDPE matrix. For the 50/50 HDPE/EVA blend, both dispersed and continuous EVA phases can be seen. For the 30/70 HDPE/EVA blend, HDPE and EVA form a cocontinuous morphology. The D_n , D_w , and D_v values of the blends were calculated, and the values are given in Table II. From the table, it is clear that as the EVA content in the blend increases, the size of the dispersed EVA domains increases. The pronounced variation of $\tan \delta$ at high concentrations of EVA is due to the higher contribution of $\tan \delta_{\max}$ from the EVA phase.

Theoretical modeling of the dynamic mechanical properties

The applicability of various composite models, such as the parallel, series, Halpin–Tsai, Coran, Takayanagi, and Kerner models, is examined to predict the dynamic mechanical behavior of the blends.

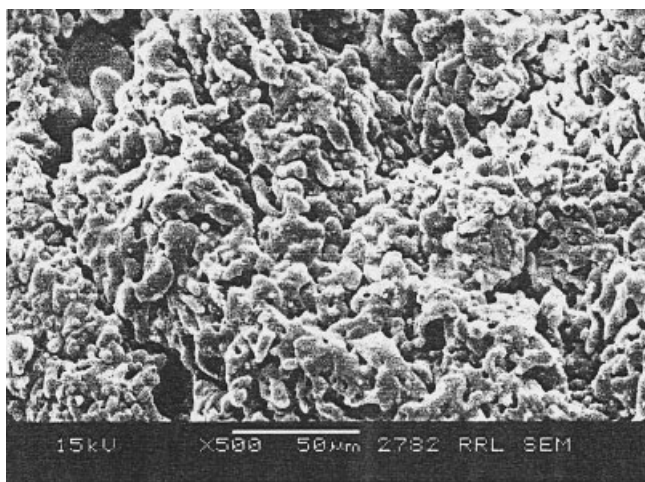


Figure 7 Scanning electron micrograph of 30/70 HDPE/EVA blends.

TABLE II
Dispersed Domain Diameters of HDPE/EVA Blends

| HDPE/EVA blend | Domain diameter (μm) | | |
|------------------|-----------------------------------|-------|-------|
| | D_n | D_w | D_v |
| 70/30 | 4.2 | 6.02 | 7.86 |
| 50/50 | 5.62 | 7.03 | 9.05 |
| 30/70 | Cocontinuous morphology | | |
| 70/30 + 2% MA-PE | 3.67 | 5.37 | 7.51 |

The parallel model (highest upper bound model) is given by the following equation:

$$M = M_1\phi_1 + M_2\phi_2 \quad (4)$$

where M is the property of the blend and M_1 and M_2 are the corresponding properties of components 1 and 2, respectively; ϕ_1 and ϕ_2 are the volume fractions of components 1 and 2, respectively. In this model, the components are considered to be arranged parallel to each other so that the applied load stretches each of the components by the same amount.

In the lowest lower bound series model, the components are arranged in series with the applied stress:

$$1/M = \phi_1/M_1 + \phi_2/M_2 \quad (5)$$

According to the Halpin–Tsai equation,¹⁶

$$M_1/M = (1 + A_i B_i \phi_2)/(1 - B_i \phi_2) \quad (6)$$

$$B_i = (M_1/M_2 - 1)/(M_1/M_2 + A_i) \quad (7)$$

In these equations, subscripts 1 and 2 refer to the continuous and dispersed phases, respectively. The constant A_i is defined by the morphology of the system. For elastomer domains dispersed in a hard continuous matrix, A_i is 0.66.

In Coran's model, the properties are generally between the parallel model upper bound (M_U) and the series model lower bound (M_L). According to Coran's equation,¹⁷

$$M = f(M_U - M_L) + M_L \quad (8)$$

where f can vary between zero and unity. f is a function of the phase morphology and is given as follows:

$$f = V_H^n (nV_S + 1) \quad (9)$$

where n contains the aspects of phase morphology. V_H and V_S are the volume fractions of the hard phase and soft phase, respectively.

According to Takayanagi model,^{18,19}

$$M = (1 - \lambda)M_1 + \lambda[(1 - \phi)/M_1 + (\phi/M_2)]^{-1} \quad (10)$$

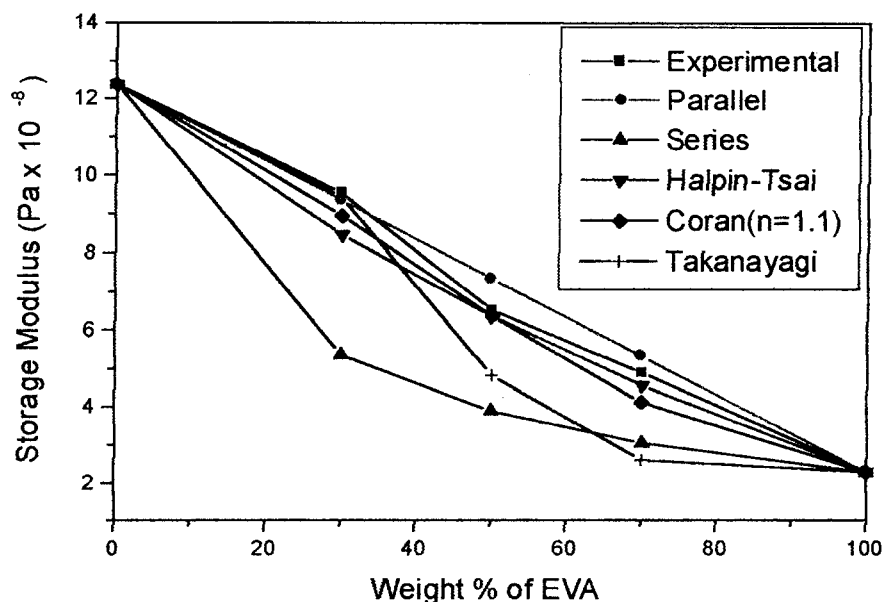


Figure 8 Experimental and theoretical values of G' of HDPE/EVA blends as a function of the EVA content in the blend at -25°C .

M_1 is the property of the matrix phase, M_2 is the property of the dispersed phase, and $\phi\lambda$ is the volume fraction of the dispersed phase and is related to the degree of series-parallel coupling. The degree of parallel coupling of the model can be expressed as follows:

$$\% \text{ parallel} = [\phi(1 - \lambda)/(1 - \phi\lambda)] \times 100 \quad (11)$$

Figure 8 shows the experimental and theoretical plots of G' of HDPE/EVA blends at -25°C as a function of the weight percentage of EVA in the blend. The G' values lie between the upper bound parallel model and lower bound series model. The experimental values are close to those of the Halpin-Tsai model above 50 wt % EVA and close to those of the Coran model up to 50 wt % EVA in the blend. For the Takayanagi model, which is widely used for the prediction of viscoelastic data, the experimental values can be described with 20% parallel coupling. The theoretical value is in good agreement with the experimental value for the 70/30 HDPE/EVA blend. However, for the 50/50 and 30/70 HDPE/EVA blends, the experimental values are higher than those calculated with the Takayanagi model. This may be because the theoretical values are calculated according to the assumption that one phase is dispersed in the other. However, for 30/70 blends, the system shows a cocontinuous morphology, and for 50/50 blends, the system shows some degree of cocontinuity.

Phase mixing in the blends

The area under the G'' -temperature curves (LA) is related to the chemical composition of the material. In

addition, it can be significantly affected by the morphology of the polymer blend system.²⁰ The quantity LA was found to be a molecular characteristic, governed by the structures of the individual polymers.²¹

The integral of the G'' -temperature curve is characterized to develop a relationship between the extent of damping and the contribution for each group in the polymeric material toward the damping performance. LA can be evaluated by the integral method, as suggested by Fay et al.²⁰ LA can be derived from the phenomenological approach:²²

$$\text{LA} = \int_{T_R}^{T_G} G'' dT \cong (G'_G - G'_R)(R/E_{\infty})(\pi/2)T_G^2 \quad (12)$$

where G'_G and G'_R are the storage moduli in the glassy and rubbery states, respectively, and T_G and T_R are the glassy and rubbery temperatures just below and above the glass transition, respectively. E_{∞} is the

TABLE III
Theoretical and Experimental Values of LA

| | Experimental (Pa K) | Theoretical (Pa K) |
|---------------------------|------------------------|-----------------------|
| 70/30 HDPE/EVA | 9.83×10^9 | 3.70×10^9 |
| 50/50 HDPE/EVA | 8.36×10^9 | 3.98×10^9 |
| 30/70 HDPE/EVA | 4.68×10^9 | 4.23×10^9 |
| 70/30 HDPE/EVA + 2% MA-PE | 1.008×10^{10} | 3.70×10^9 |
| 50/50 HDPE/EVA + 5% MA-PE | 9.02×10^9 | 3.70×10^9 |
| 30/70 HDPE/EVA + 1% MA-PE | 5.98×10^9 | 3.70×10^9 |
| 70/30 HDPE/EVA + 0.5% DCP | 1.16×10^{10} | 3.70×10^9 |
| 70/30 HDPE/EVA + 1.5% DCP | 1.26×10^{10} | 3.70×10^9 |

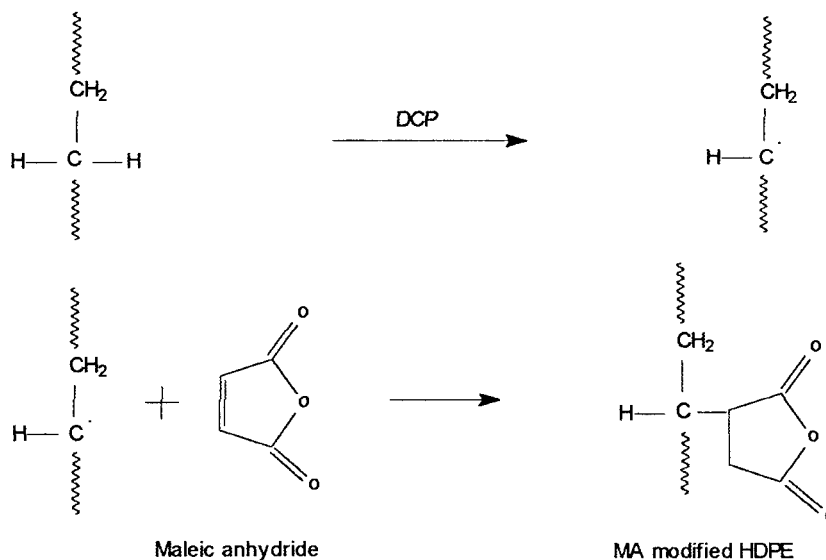


Figure 9 Schematic representation of the mechanism of grafting of MA onto HDPE.

activation energy of the relaxation process, and R is the gas constant.

To determine the theoretical values, we have used the group contribution analysis.^{21,22} This analysis helps us to select polymers with specified damping characteristics and provides a quantitative basis for developing new theories of molecular motions near T_g . It is based on the assumption that the structural groups in the repeating units provide a weight fraction additive contribution to the total loss area. The basic equation for the group contribution analysis of LA is^{21,22}

$$LA = \sum_{i=1}^n (LA)_i M_i / M = \sum_{i=1}^n G_i / M \quad (13)$$

where M_i is the molecular weight of the i th group of the repeating unit, M is the molecular weight of the whole mer, G_i is the molar loss constant for the i th group, and n represents the number of moieties in the mer. Equation (13) provides a predictive method for LA values via the structure of the polymer.

The theoretical and experimental values of LA for various blends are given in Table III. The experimental values are larger than those obtained by group contribution analysis. This is because the experimental value of LA is influenced by the morphology, the

interactions between the polymer components, and the phase continuity of the system. The higher experimental values of LA indicate enhanced interactions between the component polymers and enhanced damping. For HDPE/EVA blends, there will be some degree of compatibility, which may arise because of the structural similarities of HDPE and EVA.

Effect of compatibilization

Most of the polymer blends are generally incompatible because of the lack of physical and chemical interactions across the phase boundaries and poor interfacial adhesion. The properties of these immiscible polymer blends can be improved by the addition of compatibilizers or interfacial agents.⁵ The addition of suitably selected compatibilizers to immiscible polymer blends should (1) reduce the interfacial energy of the two phases, (2) permit finer dispersion during mixing, (3) reduce coalescence during mixing and further processing, and (4) result in improved interfacial adhesion.²³ In polymer blends, the mechanical properties are always affected by the morphology of the blends.²⁴⁻²⁷

For the compatibilization of HDPE/EVA blends, MA-g-HDPE was prepared and then added to the blends. The mechanism of grafting MA onto HDPE

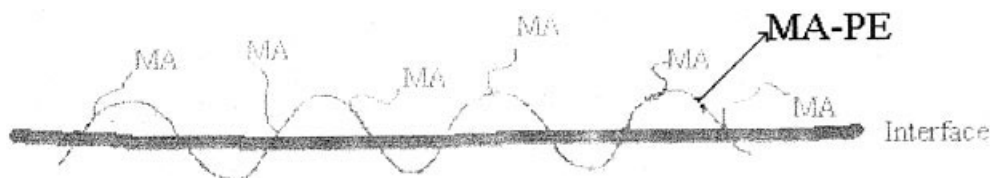


Figure 10 Schematic representation of the compatibilizing action of MA-PE on HDPE/EVA blends.

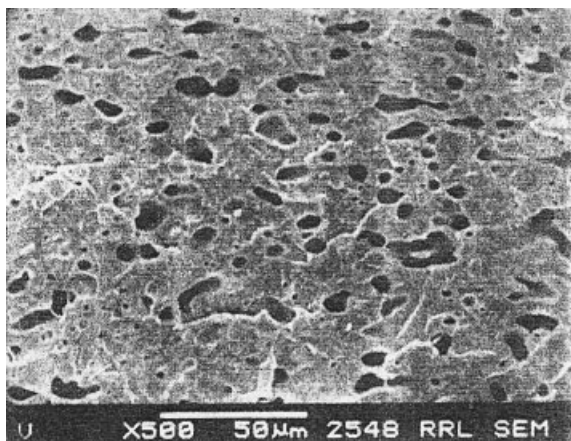


Figure 11 Scanning electron micrograph of 70/30 HDPE/EVA blends containing 2% MA-PE.

has already been reported.^{11,28} The grafting of MA onto HDPE is carried out in the presence of DCP. At high temperatures, the presence of DCP generates free radicals in the PE backbone. These free radicals react with the MA molecules, and MA is grafted onto the PE backbone; the reaction involved in the process is given in Figure 9. This grafting of MA onto the PE backbone creates a brushlike interface.²⁹ The compatibilizer is located at the interface between HDPE and EVA. The nonpolar part of the compatibilizer (PE) is wetted by the HDPE phase, and the polar part of the compatibilizer (MA) is wetted by the EVA phase because of the dipolar interaction between the MA groups of MA-PE and EVA. A schematic representation of the compatibilizing action of MA-PE on HDPE/EVA blends is given in Figure 10. This dipolar interaction causes a reduction in the domain size of the dispersed EVA

particles, which is evident from Figure 11. This reduction in the particle size with the addition of compatibilizers is due to the reduction in the interfacial tension between the dispersed EVA and continuous HDPE matrix and also due to the suppression of coalescence. The change in the domain diameter of the 70/30 HDPE/EVA blend upon compatibilization is more clear in Table II.

G' , G'' , and $\tan \delta$ of 70/30 HDPE/EVA blends compatibilized with 0.5 and 2% MA-PE are given in Figures 12–14. The addition of 0.5% MA-PE to the 70/30 HDPE/EVA blend system leads to a small increase in G' over the whole temperature range and a small increase in G'' at low temperatures (up to 0°C). The addition of 2% MA-PE leads to an increase in G' and G'' values to a considerable extent over the whole temperature range. The increase in the modulus values with the addition of 2% MA-PE is due to the increased interactions between PE and EVA in the presence of the compatibilizer.

For 0.5% MA-PE compatibilized blends, the $\tan \delta$ peak of EVA is shifted to the low-temperature region by about 2.5°C, and for 2% MA-PE compatibilized blends, the shift is about 2.2°C. The low-temperature γ relaxation of HDPE is shifted to the low-temperature region by the addition of MA-PE. The decrease is about 4.3 and 4.5°C for 0.5 and 2% MA-PE compatibilized blends, respectively. The high-temperature α relaxation of HDPE is also reduced (2.2°C) by the addition of 2% MA-PE.

In this case, the compatibilized blends show the presence of two peaks corresponding to T_g 's of HDPE and EVA similar to those of the uncompatibilized blends (Fig. 14). This indicates that the compatibiliza-

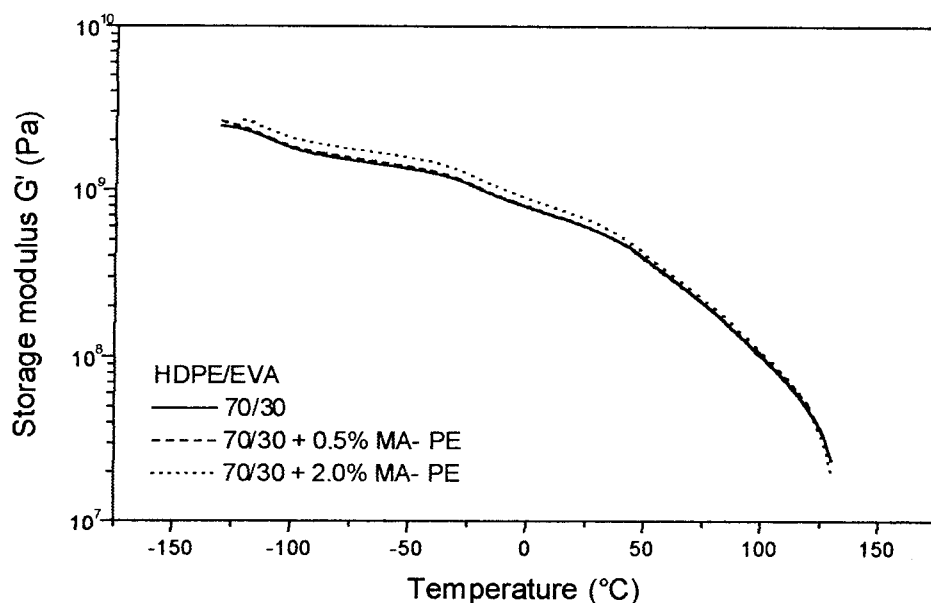


Figure 12 Dependence of G' on the temperature of 70/30 HDPE/EVA compatibilized blends.

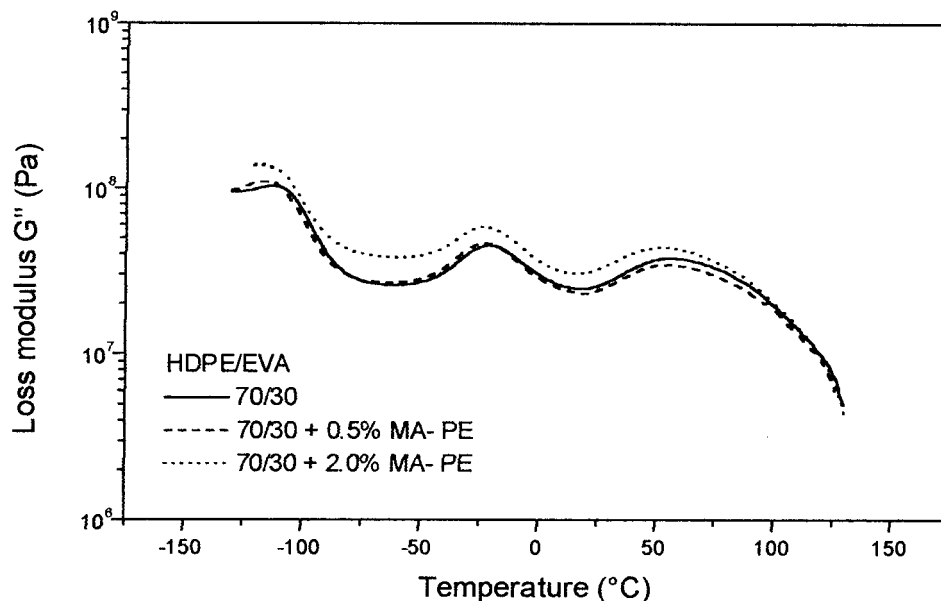


Figure 13 Dependence of G'' on the temperature of 70/30 HDPE/EVA compatibilized blends.

tion does not alter the level of miscibility, even though it causes a reduction in the particle size and a decrease in the relaxation temperature.⁶ This is in agreement with the conclusions made by Paul and Newman,⁵ who suggested that if two polymers are far from being miscible, then no compatibilizer is likely to make a one-phase system, and in a completely immiscible system, the main role of the compatibilizer is to act as an interfacial agent.

The addition of 0.5% MA-PE has only a small effect on the $\tan \delta$ values of the blends. For 2% MA-PE, the $\tan \delta$ values are considerably higher than those of the uncompatibilized blends up to room temperature, but

at high temperatures, the effect is not much pronounced. This change in $\tan \delta$ with temperature indicates that the interfacial interaction caused by the presence of MA-PE in the blend may be weakened at higher temperatures. The decrease in interfacial interactions at high temperatures will reduce the interfacial adhesion and, therefore, lead to increased segmental motion. The most obvious changes due to compatibilization are the higher values in $\tan \delta$ and G'' in the region between the relaxation temperatures of HDPE (-110°C) and EVA (-20°C). This indicates improved interactions between HDPE and EVA phases in the presence of MA-PE.

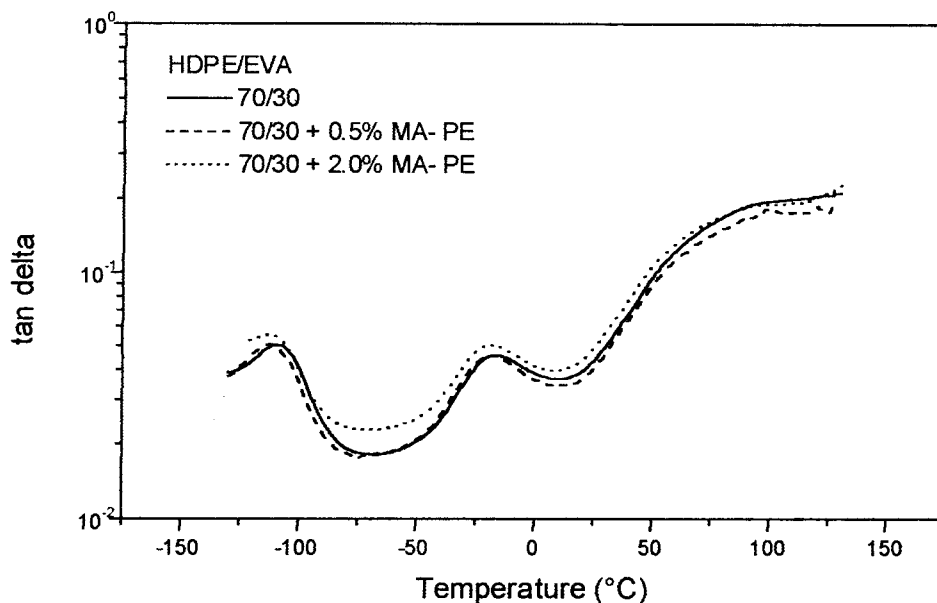


Figure 14 Dependence of $\tan \delta$ on the temperature of 70/30 HDPE/EVA compatibilized blends.

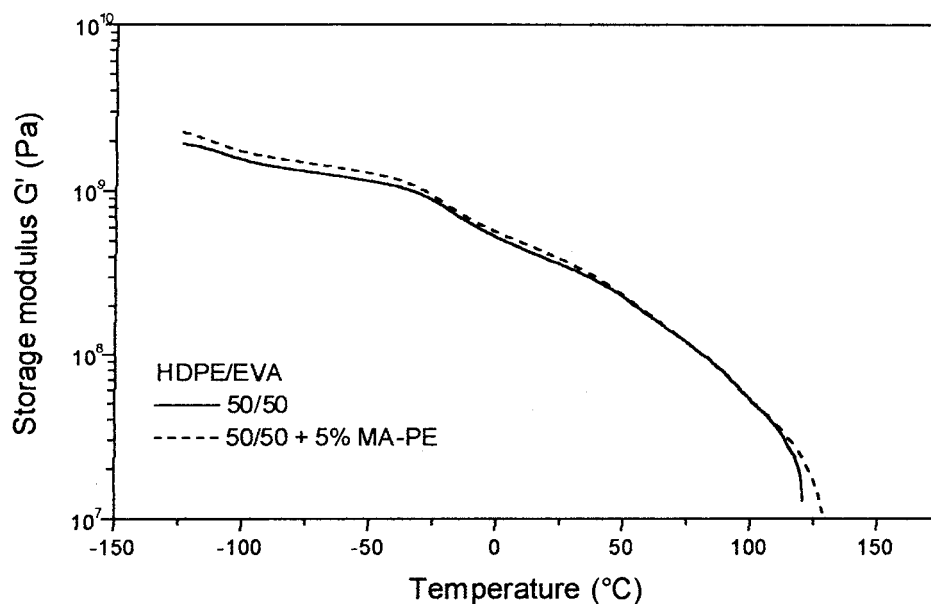


Figure 15 Dependence of G' on the temperature of 50/50 HDPE/EVA compatibilized blends.

Figures 15–17 represent the variations of G' , G'' , and $\tan \delta$ of 50/50 HDPE/EVA blends compatibilized with 5% MA-PE. G' and G'' of the sample increase upon compatibilization over the whole temperature range (Figs. 15 and 16). For compatibilized blends, the intensities of $\tan \delta$ peaks are slightly higher than those of the uncompatibilized blends up to T_g of EVA (Fig. 17). However, at high temperatures, the intensities of $\tan \delta$ peaks are lower than those of uncompatibilized blends. The increase in modulus and $\tan \delta$ values upon compatibilization is due to the increased interaction between the HDPE and EVA phases in the presence of the compatibilizer. The γ -relaxation tem-

perature of HDPE is shifted to the low-temperature region by about 2.5°C after the addition of 5% MA-PE. The α -relaxation temperature of HDPE is also decreased. The $\tan \delta$ peak of EVA is shifted to the low-temperature region by about 5°C. The intensity of the $\tan \delta$ peak corresponding to the EVA content is slightly decreased, and the peak appears sharper because of a higher loss in intensity in the range between the relaxation temperature and 30°C.

G' , G'' , and $\tan \delta$ of 30/70 HDPE/EVA blends compatibilized with 1% MA-PE are given in Figures 18–20. The addition of 1% MA-PE increases the modulus and $\tan \delta$ values of the compatibilized blends slightly

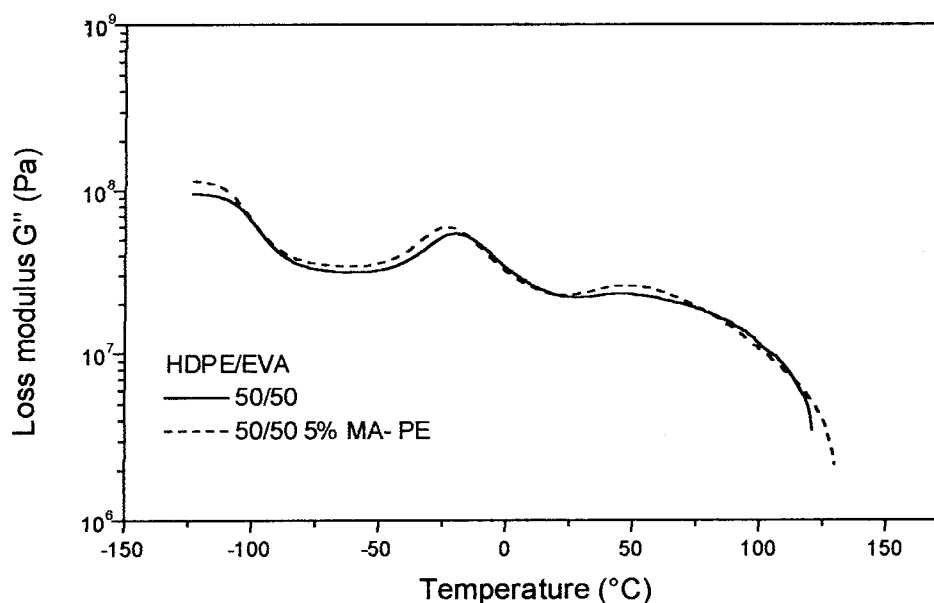


Figure 16 Dependence of G'' on the temperature of 50/50 HDPE/EVA compatibilized blends.

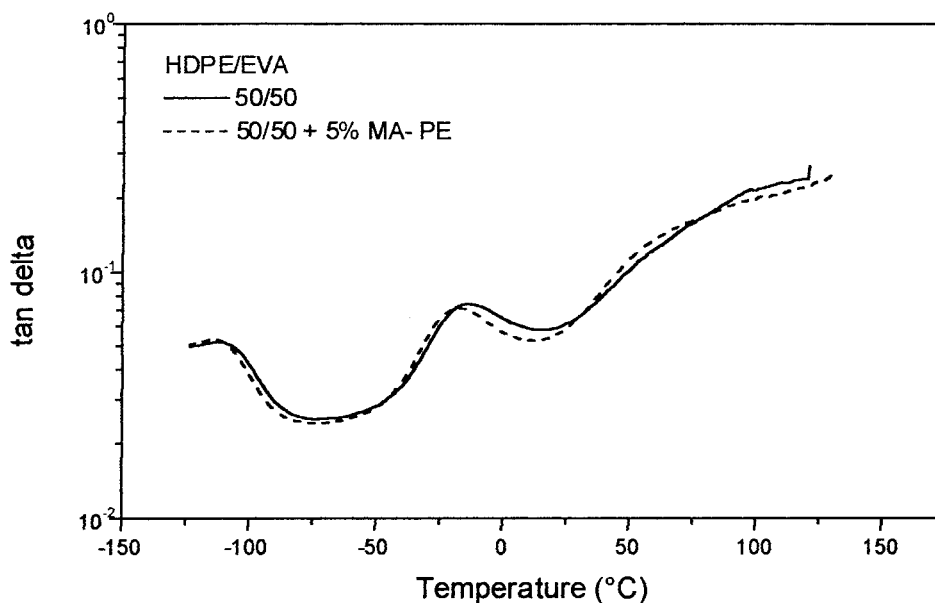


Figure 17 Dependence of $\tan \delta$ on the temperature of 50/50 HDPE/EVA compatibilized blends.

up to -50°C . In both compatibilized and uncompatibilized blends, the relaxation of HDPE is not clear because of the small amounts of HDPE in the blend. The intensity of the $\tan \delta$ peak corresponding to the EVA phase is slightly decreased, and the peak appears sharper because of the higher loss in intensity in the temperature range of -20 (the relaxation temperature of EVA) to 30°C , which is similar to that of the 50/50 blend. The α -relaxation behavior of HDPE is more clearly visible in the $\tan \delta$ -temperature and G'' -temperature curves in comparison with uncompatibilized blends.

For the 70/30 and 50/50 HDPE/EVA blends, the relaxation temperatures of HDPE and EVA are shifted

to lower temperatures upon compatibilization, and this indicates an increased penetration of the two phases.¹⁰ However, for the 30/70 HDPE/EVA blend, the addition of a compatibilizer does not change the relaxation temperature, and this may be due to the cocontinuous morphology of the blends. In the 50/50 and 30/70 compatibilized blends, the intensity of the relaxation peak corresponding to EVA is reduced and becomes sharper because of the higher loss in intensity in the range between the relaxation temperature of EVA (-20°C) and 30°C .

For compatibilized blends, LA is greater than that of the corresponding uncompatibilized blends (Table II).

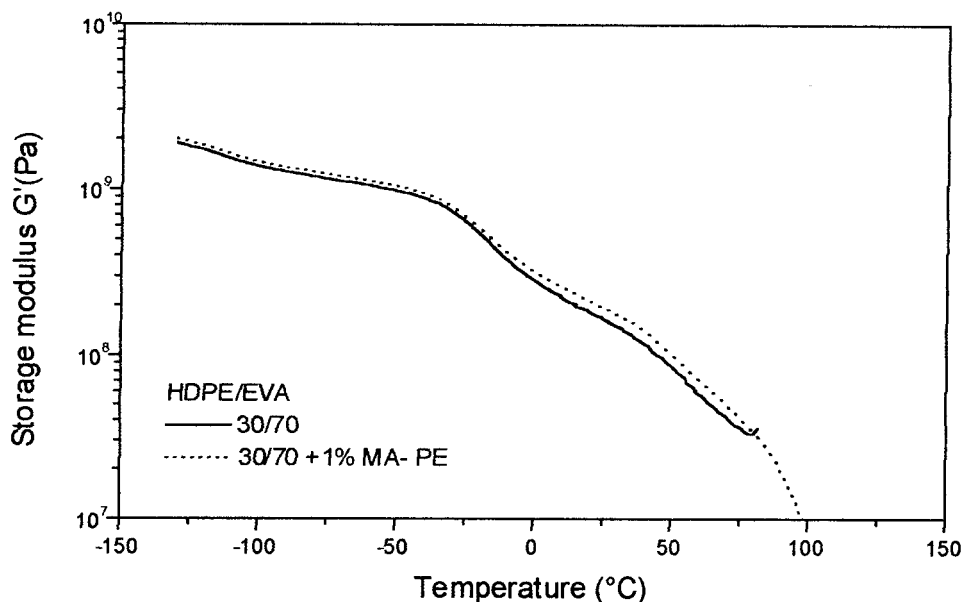


Figure 18 Dependence of G' on the temperature of 30/70 HDPE/EVA compatibilized blends.

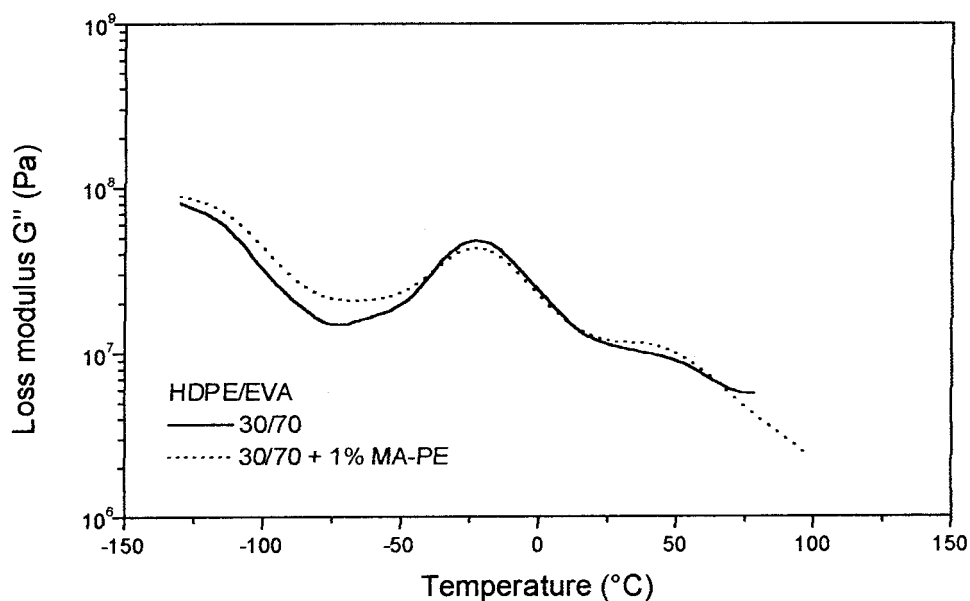


Figure 19 Dependence of G'' on the temperature of 30/70 HDPE/EVA compatibilized blends.

This increase in LA of compatibilized blends indicates enhanced interactions between the HDPE and EVA phases in the presence of the compatibilizer.

Effect of dynamic vulcanization

The vulcanization of the rubbery phase during mixing has been investigated as a way to improve the physical properties of several thermoplastic elastomers based on rubber/plastic blends. The change in morphology that occurs during dynamic vulcanization is schematically represented in Figure 21. During dynamic vulcanization, a cocontinuous morphology may

be transferred to a matrix and dispersed-phase morphology, there may be some possibility of phase inversion, or the crosslinked rubber phase may become finely and uniformly dispersed in the plastic matrix. During the process of dynamic vulcanization, the viscosity of the rubber phase increases because of crosslinking, and the rubber domains can no longer be sufficiently deformed by the local shear stress and are eventually broken down into small droplets.

The variations of G' , G'' , and $\tan \delta$ of 70/30 HDPE/EVA blends crosslinked with 0.5 and 1.5% DCP are given in Figures 22–24. The addition of peroxide to 70/30 HDPE/EVA blends leads to an increase in G'

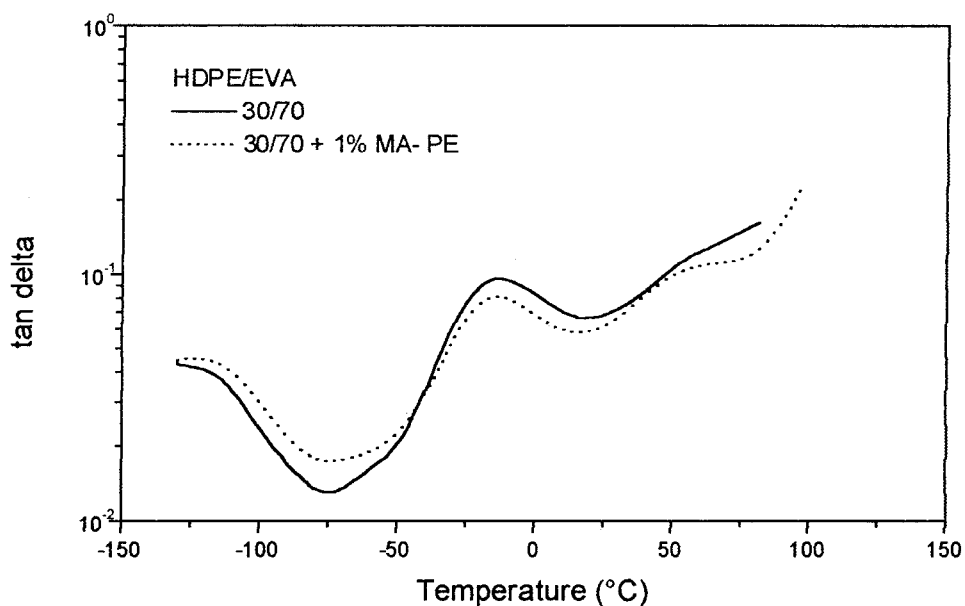
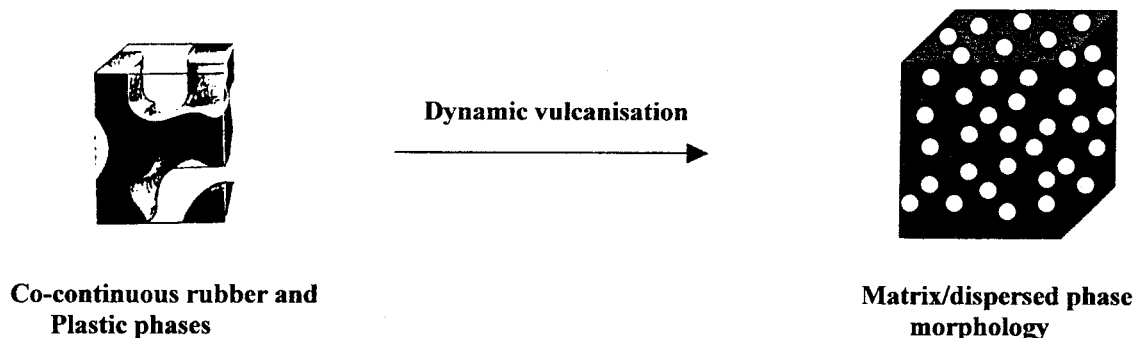
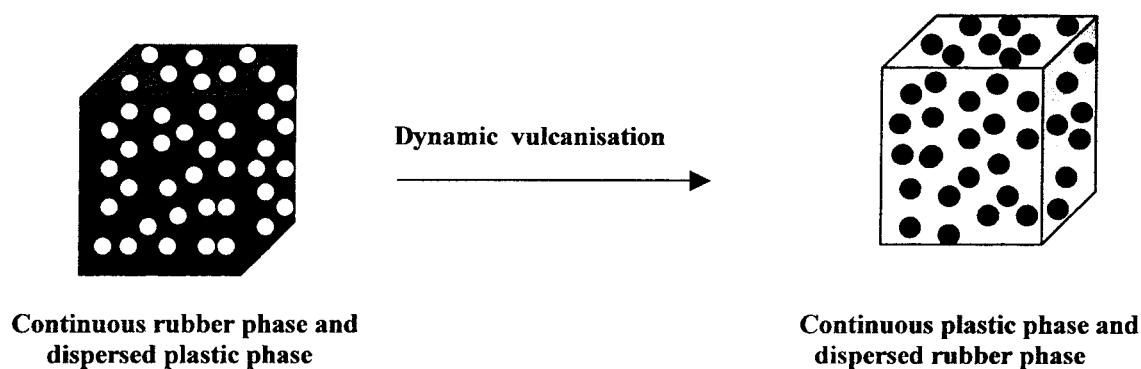


Figure 20 Dependence of $\tan \delta$ on the temperature of 30/70 HDPE/EVA compatibilized blends.

Co-continuous morphology could be transferred in to Matrix /dispersed phase morphology



Possibility of phase inversion



Finer dispersion of dispersed rubber domains

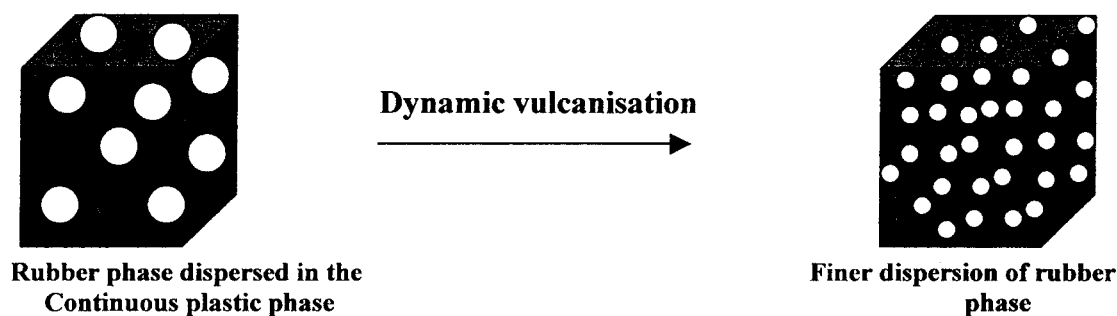


Figure 21 Schematic representation of the dynamic vulcanization.

and G'' . This increase is more pronounced at the higher DCP contents. At temperatures greater than 100°C , 1.5% DCP leads to a decrease in G' . The α - and γ -relaxation temperatures of HDPE are not influenced significantly by the addition of DCP. The relaxation of EVA at about -20°C is slightly changed by the addition of 0.5% DCP. The addition of 1.5% DCP leads to significant increase in the relaxation temperature of EVA by 3.6 K, which indicates the predominant

crosslinking of the EVA phase. In addition, the intensity of the $\tan \delta$ peak corresponding to the EVA content increases with the increase in the DCP content. In this case also, the blends show the presence of two peaks corresponding to T_g 's of HDPE and EVA, which indicates the immiscibility of the system. The peak widths at the half-heights of the 70/30 HDPE/EVA blend and the 70/30 HDPE/EVA blends crosslinked with 0.5 and 1.5% DCP were 31, 33, and 37°C , respec-

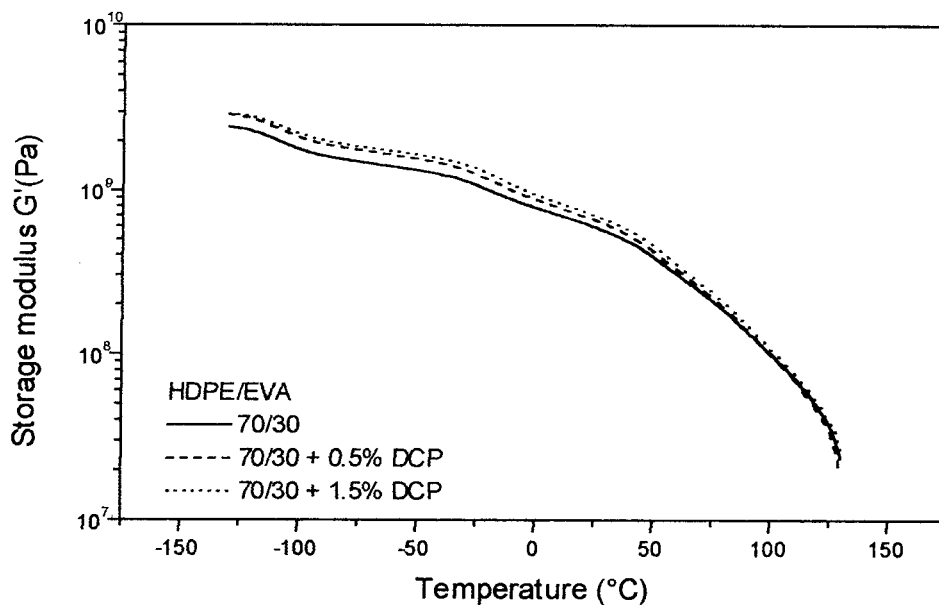


Figure 22 Dependence of G' on the temperature of 70/30 HDPE/EVA dynamically crosslinked blends.

tively. This increase in the peak width or broadening of peaks upon crosslinking indicates that dynamic crosslinking promotes interfacial bonding between the phases,⁷ which may arise because of the crosslinking of HDPE and EVA phases. Dynamic crosslinking has been reported⁵ as a means of imparting interfacial bonding (compatibility) between the phases in EPDM/PP and NR/PP blends.

For crosslinked blends, LA is also greater than LA of the corresponding uncrosslinked blends (Table II). This increase in LA of crosslinked blends indicates enhanced interactions between the HDPE and EVA phases during crosslinking.

CONCLUSIONS

The effects of the blend ratio, reactive compatibilization, and dynamic vulcanization on the dynamic mechanical properties of HDPE/EVA blends have been analyzed in the temperature range of -130 to 150°C with a dynamic mechanical thermal analyzer. G' of the blends decreases with an increase in the EVA content in the blends. For HDPE, $\tan \delta_{\text{max}}(T_g)$ occurs at -110°C , and for EVA, it occurs at -15°C . During blending, T_g 's corresponding to both HDPE and EVA shift to low-temperature regions. The $\tan \delta$ curves show two peaks, corresponding to HDPE and EVA,

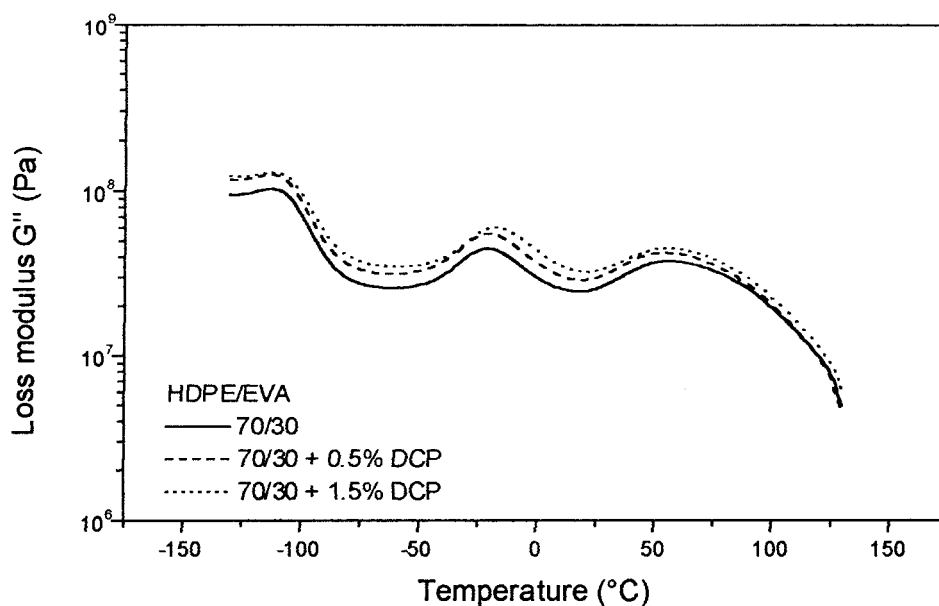


Figure 23 Dependence of G'' on the temperature of 70/30 HDPE/EVA dynamically crosslinked blends.

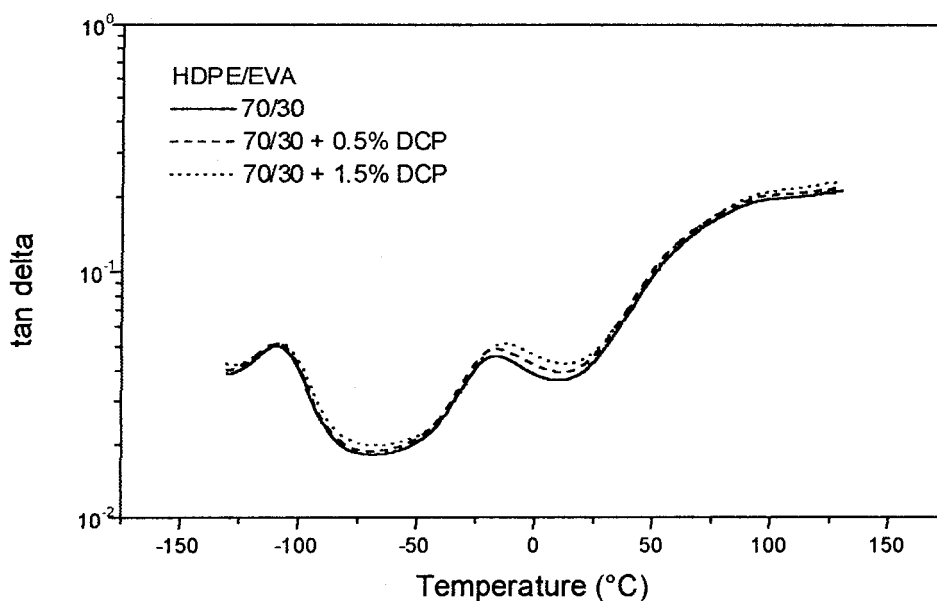


Figure 24 Dependence of $\tan \delta$ on the temperature of 70/30 HDPE/EVA dynamically crosslinked blends.

indicating the immiscible and incompatible nature of the system. The immiscible nature of the system is also evident from the morphology of the blends. The phase morphology of the blends indicates that for 70/30 blends, the EVA phase is dispersed as spherical domains in the continuous HDPE matrix, and for 50/50 HDPE/EVA blends, the system shows dispersed and continuous EVA phases. For 30/70 HDPE/EVA blends, HDPE and EVA form cocontinuous phases.

Various theoretical models have been used to predict the dynamic mechanical behavior of the blends at $-25 \pm 1^\circ\text{C}$. This temperature has been selected because the relaxation of EVA occurs at -24°C and there is a rapid fall in the G' values around this temperature. The experimental values are close to those of the Halpin-Tsai model above 50 wt % EVA and close to those of the Coran model up to 50 wt % EVA in the blend. For the Takayanagi model, which is widely used for the prediction of viscoelastic data, the theoretical value is in good agreement with the experimental value for the 70/30 HDPE/EVA blend. However, for the 50/50 and 30/70 HDPE/EVA blends, the experimental values are higher than those calculated with the Takayanagi model.

LA has been analyzed with the integration method from the experimental curve and has been compared with those values obtained from group contribution analysis. The LA values calculated with group contribution analysis are lower than those obtained from experimental data (the integration method). This is because the morphology, the interactions between the polymer components, and the phase continuity influence the experimental values of LA. Because HDPE and EVA have some structural similarities, there is a marginal level of interaction between HDPE and EVA.

For the 70/30 and 50/50 blends, the addition of the MA-PE compatibilizer shifts the relaxation temperatures of both HDPE and EVA to lower temperatures, and this indicates the increased penetration of the two phases upon compatibilization. The increased interaction of the HDPE and EVA phases upon compatibilization can be explained with the morphology of the compatibilized blend. The compatibilizer reduces the interfacial tension between the dispersed EVA phase and continuous HDPE phase, and this results in the reduction of the particle size. However, for the 30/70 HDPE/EVA blend, the addition of the compatibilizer does not change the relaxation temperature significantly, and this may be due to the cocontinuous morphology of the blends. The G' and G'' values of the compatibilized blends are higher than those of the uncompatibilized blends. In the 50/50 and 30/70 compatibilized blends, the intensity of the relaxation peak corresponding to EVA is reduced and becomes sharper because of the higher loss in intensity in the range between the relaxation temperature of EVA (-20°C) and 30°C .

The dynamic vulcanization of the EVA phase leads to small changes in the relaxation behavior of the system, especially in the EVA phase of the blends. The G' , G'' , and $\tan \delta$ values increase during vulcanization. The addition of 1.5% DCP leads to a significant increase in the relaxation temperature of EVA by 3.6 K, which indicates the predominant crosslinking of the EVA phase. The peak width at the half-height of the $\tan \delta$ curves increases during crosslinking. This broadening of $\tan \delta$ peaks of crosslinked blends indicates an increased interaction between the two phases during vulcanization.

The effect of compatibilization and dynamic vulcanization on the HDPE/EVA blends can be explained with LA. For compatibilized and crosslinked blends, LA is greater than that of the corresponding uncompatibilized HDPE/EVA blends. This increase in LA of the compatibilized and crosslinked blends indicates an enhanced interaction between the HDPE and EVA phases during compatibilization and crosslinking.

References

1. Dynamic Mechanical Analysis of Polymeric Materials; Murayama, T. M., Ed.; Elsevier: New York, 1978.
2. Cho, K.; Ahn, T. K.; Lee, B. H.; Choe, S. *J Appl Polym Sci* 1997, 63, 1265.
3. Karger-Kocsis, J.; Kiss, L. *Polym Eng Sci* 1987, 27, 254.
4. Varughese, H.; Bhagawan, S. S.; Rao, S. S.; Thomas, S. *Eur Polym J* 1996, 1, 957.
5. Paul, D. R.; Newman, S., Eds.; Academic: New York, 1978.
6. Zhang, Z. Q.; Chen, H.; Tang, T.; Huang, B. H. *Macromol Chem Phys* 1995, 196, 3585.
7. Thomas, S.; George, A. *Eur Polym J* 1992, 28, 1451.
8. Koshy, A. T.; Kuriakose, S.; Thomas, S.; Varghese, S. *Polymer* 1993, 34, 3428.
9. George, S.; Neelakantan, N. R.; Varughese, K. T.; Thomas, S. *J Polym Sci Part B: Polym Phys* 1997, 35, 2309.
10. John, B.; Oommen, Z.; Varughese, K. T.; Thomas, S. *Polymer*, submitted.
11. Coran, A. Y.; Patel, R. *Rubber Chem Technol* 1983, 56, 1045.
12. Ward, I. M.; Harley, D. W. *An Introduction to the Mechanical Properties of Solid Polymers*; Wiley: New York, 1993; p 184.
13. *Kunststoff Handbuch*; Hanser: Munich, 1969; p 212.
14. Varughese, K. T.; Nando, G. B.; De, P. P.; De, S. K. *J Mater Sci* 1988, 23, 3894.
15. Thomas, S.; Gupta, B. R.; De, S. K. *J Vinyl Technol* 1987, 9, 71.
16. Nielson, L. E. *Rheol Acta* 1974, 13, 86.
17. Coran, A. Y. In *Hand Book of Elastomers*; Bhowmick, A. K.; Stephens, H. L., Eds.; Marcel Dekker: New York, 1988; p 249.
18. Dickie, R. A. *J Appl Polym Sci* 1973, 17, 45.
19. Holsto-Miettiner, R. M.; Seppala, J. Y.; Ikkala, O. T.; Reima, I. T. *Polym Eng Sci* 1994, 34, 395.
20. Fay, J. J.; Thomas, D. A.; Sperling, L. H. *J Appl Polym Sci* 1991, 43, 1617.
21. Chang, M. C. O.; Thomas, D. A.; Sperling, L. H. *J Polym Sci Polym Part B: Polym Phys* 1987, 26, 1627.
22. Chang, M. C. O.; Thomas, D. A.; Sperling, L. H. *J Appl Polym Sci* 1987, 34, 409.
23. Paul, D. R.; Barlow, G. W. *Adv Chem Ser* 1979, 176, 315.
24. Schmitt, B. J. *Angew Chem* 1979, 91, 286.
25. Wu, S. *Polymer* 1985, 26, 1855.
26. Potschke, P.; Wallheinke, K.; Fritsche, H.; Stutz, H. *J Appl Polym Sci* 1997, 64, 762.
27. Potschke, P.; Wallheinke, K.; Stutz, H. *J Polym Eng Sci* 1999, 39, 1035.
28. George, J.; Joseph, R.; Thomas, S.; Varughese, K. T. *J Appl Polym Sci* 1995, 57, 449.
29. Gatenholm, P.; Felix, J. M. In *New Advances in Polyolefins*; Chung, T. C., Ed.; Plenum: New York, 1993.